Research article

Explore the multitarget mechanism of tetrahydrocurcumin preventing on UV-induced photoaging mouse skin

Chuan Xu [a], Qian-Wei Xiong [d], Yue Li [c], Jun-Ning Zhao [b], Lu Zhang [b], Xiao-Lu Li [b,c,*]

[a] Department of Oncology, The General Hospital of Western Theater Command, Chengdu, China
[b] Translational Chinese Medicine, Key Laboratory of Sichuan Province, Sichuan Academy of Chinese Medicine Sciences, Sichuan Institute for Translational Chinese Medicine, China
[c] Department of Plastic and Burn Surgery, National Key Clinical Construction Specialty, The Affiliated Hospital of Southwest Medical University, China
[d] Bravou Plastic Surgery Hospital, China

ABSTRACT

UV induced photoaging is the main external factor of skin aging. In this study, we tested the protective effects of tetrahydrocurcumin on UV-induced skin photoaging of KM mice and researched the multi-target mechanism through RNA sequencing technology. Mouse experiments show that tetrahydrocurcumin strongly changed in skin appearance, epidermal thickness, and wrinkle-related parameters in UV-irradiated mice. RNA-seq result show that we found 29 differentially expressed mRNA transcripts in UV mice relative to Ctrl rats (18 up-regulated and 11 down-regulated) and 7 significantly dysregulated mRNAs were obtained in the THC group compared to the UV group (1 up-regulated and 6 down-regulated), respectively. Spink7, Edn3, Stab2 may be the key target genes of tetrahydrocurcumin in preventing aging. Bioinformatics analysis shows that the response to muscle contraction and melanin biosynthetic GO term and Inflammation related pathway such as PPAR, MAPK would involve in effects of tetrahydrocurcumin. The results of this study indicated that tetrahydrocurcumin can improve the appearance through anti-inflammatory, improving extracellular matrix and inhibiting melanin production. It could be suggested as a protective measure in the prevention of UV-induced photoaging.

1. Introduction

In recent years, due to severe light pollution, ozone destruction has caused a significant increase in the dose of UV radiation reaching the surface UV-induced skin damage, inflammation and other problems have received wider attention. Ultraviolet (UV) radiation has been recognized as the major external invasion cause of photoaging [1, 2], photoaging skin become erythema, roughens, laxity, wrinkled, lack of luster and increase the risk of skin disease [3, 4]. The major solar UV radiation reaching the earth consists of a combination of UVB (290–320 nm) and UVA (320–400 nm) wave length [5]. UVA has a strong penetrating ability that can affect the dermis, such as formation of wrinkles, loss of skin tone and reduced elasticity [6, 7]. UVB can directly interact with DNA to produce thymine dimer photoproduct, resulting in erythema and sunburn [1, 8]. UV radiation produces ROS that cause destructive oxidative stress, damage the structure and function of cells, mediate inflammatory responses [9], reduce collagen and elastic fibers is reflected [10, 11, 12].

Pervious extensive publications have suggested that many natural products have demonstrated protective and anti-aging effects on the skin through ROS scavenging, including Kuding Tea, vaccinium uliginosum, curcumin, asiaticoside, etc. [13, 14, 15]. Natural antioxidants are favored for their simplicity, safety, effectiveness. Curcumin, a natural polyphenolic and yellow pigment obtained from the spice turmeric, which has been shown to prevent and treat of parasitic skin infections, infected wounds, premature aging, inflammation, and psoriasis [16]. Whereas, curcumin's poor bioavailability, low aqueous solubility, chemical instability, rapid degradation, and rapid systemic elimination as major limitations for its use in clinical practice [17].

Tetrahydrocurcumin (THC) is the polyphenolic compounds, the main metabolite of curcumin, it was widely concerned because of its have strong antioxidant, anti-inflammatory, physiological stability and are easily absorbed through the gastrointestinal tract [18, 19, 20]. In addition, numerous studies also reported that other skin-related benefits of THC such as acceleration of wound healing by reducing the epithelialization

time, as well as promotion of collagen production in the dermis, etc. [21, 22]. However, to our knowledge, in vivo experiments study on the effects and mechanism of THC on skin aging have not been performed. This study we used photoaging animal model, histochemical, ELISA, and RNA-seq analysis the protective effect and molecular mechanisms of THC on skin photoaging.

2. Material methods

2.1. Animals

Female Kunming (KM) mice (n = 36; weight: 18–22g) were purchased from Sichuan Academy of Chinese Medicine Sciences (Chengdu, China). Food and water were provided ad libitum and the experimental animals were living in standard condition (temperature 20–25 °C humidity 40–60%). All experimental procedures were approved by the animal ethics committee of Sichuan Academy of Traditional Chinese Medical Sciences (NO. P20190515-3).

2.2. Skin photoaging and treatment

After adapting for 7 days, all of the mice were shaved on their back (2.5 cm*3.5 cm) and randomly divided into 3 groups: (A) control group (Ctrl) (B) UVA + UVB irradiation group (UV) (C) Tetrahydrocurcumin group (THC), n = 12. The dorsal of the KM mice were irradiated with UVA + UVB combined irradiation, five time a week for 10 weeks, except the Ctrl group. For UV exposer, a UV irradiator (FZ-A, Shi Da Photoelectric Technology CO., Ltd, Beijing, China) with UVA + UVB ultraviolet lamp (UVA lamp 320–400nm, UVB lamp 285–350nm, Huaqiang, Nanjing, China) were used. The dose according to the minimum erythema dose incremental method [23]: the first week was 1MED (100 mJ/cm^2), while the dose was increase to 2 MED for the second week, then 3 MED for the third week, and finally 4 MED from the fourth week to the end of the experiment. The total UV irradiation intensity were 17J/cm^2. Meanwhile, the mice in THC group were administered THC (suspended in 0.5% wt/vol CMC-Na solution) at a daily dose of 100 mg per kg bodyweight (PubChem CID:124072; purity >98%, Figure 1), 30 min before UV exposure, and the equal volume of 0.5% CMC-Na solution for control and model groups.

During the irradiation process, the back skin of each group were observed regularly on every Wednesday, and photoaging of the mice were grade according to the Bissett scoring standard (Table1) [24, 25, 26].

2.3. Histochemistry

The collected skin tissues were fixed in 4% buffered formalin for 24h, then dehydrated, cleared, infiltrated, embedded in paraffin, and cut into 4 μm thick serial sections with hematoxylin and eosin (H & E), Masson's trichrome, Verhoeff prior to microscopy (DFC295; Leica, 公司, Germany).

2.4. Enzyme-linked immunosorbent assay (ELISA)

The concentrations of superoxide dismutase (SOD), glutathione peroxidase (GSH-Px), hydroxyproline (HYP) and malondialdehyde

Table 1. Grading Scale for evaluation of photoaging mice.

Grand	Evaluation criteria
0	No wrinkles or laxity; fine striations running the length of the body
1	Fine striations
2	Disappearance of all fine striations
3	Shallow wrinkles
4	a few deep wrinkles and laxity
5	increase deep wrinkles
6	Severe wrinkles, development of tumors/lesions

(MDA) in skin tissue were determined using commercially available ELISA kits (Jiang Cheng, Nanjing, China) according to the manufacturer's instructions.

2.5. RNA extraction and qualification

After 10 weeks, skin tissues were stripped out quickly from the back for RNA-seq Extract. Total RNA of each sample was extracted using TRIzol reagent (Invitrogen, U.S.) according to the manufacturer's instructions. Furthermore, 2% agarose gels were used to ensure that RNA was not degraded or contaminated. RNA concentration was measured using the Qubit RNA Assay Kit (Invitrogen, U.S.) and RNA integrity was evaluated by the RNA Nano 6000 Assay Kit of the Bioanalyzer 2100 system (Agilent Technologies, CA, USA). To ensuring the purity and quality of RNA, the value of OD 260/OD 280 was in the range of 1.8–2.1 and the value of RNA integrity number was greater than 6.8.

2.6. Illumina HiSeq sequencing

Nine cDNA libraries were constructed in this study, three from Ctrl group, UV group, and THC group. First, the rRNA was depleted using Ribo-Zero TM rRNA Removal Kit (Epicentre, U.S.) according to the manufacturer's instructions. Second, rRNA-depleted RNA was fragmented, reverse transcribed into cDNA and ligated with NEBNext adaptor using NEBNext Ultra Directional RNA Library Prep Kit for Illumina (NEB, U.S.) according to the manufacturer's recommendations. Third, the cDNA libraries purified with AMPure XP system (Beckman, Coulter, Beverly, U.S.) were enriched via PCR amplification with Phusion high-fidelity DNA polymerase, universal PCR primers, and index (X) primer. Then the library was qualified by the Qubit2.0 Fluorometer, and the clustering of the index-coded samples was performed on a cBot Cluster Generation System using HiSeq PE Cluster Kit v4 cBot (Illumina, U.S.). After cluster generation, the libraries were sequenced on an Illumina NovaSeq 6000 platform at the Novogene Bioinformatics Institute (Beijing, China) and the raw reads were generated.

2.7. Mapping to the reference genome

Clean data were obtained after filtering out the reads connected with adaptors or contented the unknown base >10%, and other low-quality reads from raw data. The Q20, Q30, and GC contents of the clean reads were calculated to ensure high-quality of all downstream analyses. Then
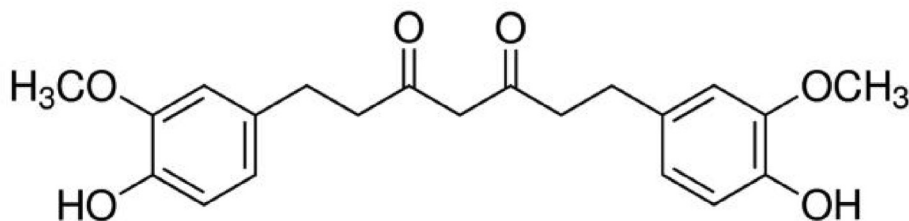

Figure 1. Chemical structures of tetrahydrocurcumin.

the reference genome and gene model annotation files were downloaded from genome website directly. Index of the reference genome was built using Bowtie2 (v2.0.5) and paired-end clean reads were aligned to the reference genome using Hisat2 (v2.0.5).

2.8. mRNA expression analysis

The mRNA expression levels in each sample were estimated according to fragments per kilo-base of exon per million fragments mapped (FPKMs) and performed using the DESeq2 R package (1.20.0). Transcripts with an adjusted p < 0.05 were assigned as differentially expressed.

2.9. Functional annotation analysis

The Gene Ontology (GO) database was used to analyze the genes enrichment of the differential mRNAs, including molecular function, cellular component, and biological process information. GO analysis was implemented by the GO seq R package (cluster Profile). GO terms with corrected P < 0.05 were considered significantly enriched.

Kyoto encyclopedia of genes and genomes (KEGG) database was used to analyze the genes enrichment of differentially expressed mRNAs. KEGG analysis was performed with cluster Profiler R package (3.8.1) through a hypergeometric test. A hypergeometric P < 0.05 was considered significantly enriched.

2.10. Quantitative real-time PCR validation

The accuracy of the sequencing mRNAs was validated through quantitative real-time PCR (qRT-PCR). The mRNAs were reverse transcribed using a TURE script 1st Stand cDNA SYNTHESIS Kit (Aid lab Bioscience, China), and qRT-PCR was performed using SYBR Green PCR Master Mix (DBI Biotechnology, China) via the Light Cycler 480 real-time PCR system following the conditions: 95 °C for 3 min, followed by 40 cycles of 95 °C for 10s and 58 °C for 30s. The specific quantitative primers were designed using Beacon Designer software and listed in Table 2. The GAPDH was used as an endogenous control for quantitative detection of the candidate mRNAs. Each experiment was performed in triplicate. The expression levels were calculated with the method of $2^{-\triangle\triangle Ct}$.

2.11. Data availability

The RNA-seq data have been deposited in the Gene Expression Omnibus database, with accession code PRJNA793231. All other data is available from the author upon reasonable request.

2.12. Statistical analysis

Statistical analysis was performed using SPSS 26.0 software. All data were expressed as mean ± SEM. Between-group comparisons were analyzed using Rank sum test or one-way AVOVA used for measurement. Independent T-test was used to compare the qPCR results. P < 0.05 was considered as statistical significance.

3. Result

3.1. THC treatment improved photoaging appearance

The result in Figure 2A demonstrated that 10 weeks after UV irradiation, visible signs of thickened and hardened, wrinkles, severe crusting of skin lesions on the dorsal skin of mice were noticed. The skin of THC group was delicate, no redness, swelling and scab were observed as compared to UV group. The Bissett score were found to be significantly decrease in the skin of the THC group compared to the UV group after 5 weeks (P < 0.01) (Figure 2B). These results indicated that THC normalize photoaging mice.

Table 2. Primer information.

Serial number	Primers	5′to3′	TM
1	GAPDH-F	GTGGTGAAGCAGGCATCT	60
	GAPDH-R	GGTGGAAGAGTGGGAGTTG	
2	Stfa3-F	CCACACCAGAAATCCAGAT	60
	Stfa3-R	CCAGCAACGACTTGAGAT	
3	Stab2-F	CAAGATATGGCAAGTTCAGAT	60
	Stab2-R	TGGTGTATGGCTCATCAATA	
4	Krt77-F	TCAACCGTAACATCCAGAG	60
	Krt77-R	CCGCATCAGAAATCAATCC	
5	Mrgprb11-ps-F	ATTCTCAGCACCATTAGCA	60
	Mrgprb11-ps-R	GCAAGGAACAGGTTACAGA	
6	Rpl34-F	TACAACACAGCCTCTAACAA	60
	Rpl34-R	TGCTTTCCCAACCTTCTT	
7	Atg9b-F	CGTGGATTACAATGTTCTCTT	60
	Atg9b-R	AATGGCATCTGACAAGGT	
8	Spink7-F	CTCTTCGCAGCAACCTAT	60
	Spink7-R	CTTCTTGTATATGTCACAGTCC	
9	Edn3-F	TTGCGTTGTACTTGTATGG	60
	Edn3-R	GAATAACTGGTGACATCTCTG	
10	Trnp1-F	GGAAGGAGGCACATTTAC	60
	Trnp1-R	GGAACTGAGTCGCTATACA	
11	Fcgbp-F	GATGTGATGGTTGGTGATG	60
	Fcgbp-R	ACTTCTCTATCGGTGTCTTC	
12	Clca3a2-F	CCTTCAGTATGGACAGTGT	60
	Clca3a2-R	TACGCAAGTTATCAGTGAGT	

3.2. THC treatment improved skin tissue structure, collagen fibers and elastic fiber's structure

HE stains showed the epidermis of the UV group was significantly thickened, some cells were blurred, the nucleus were dissolved, many inflammatory cells were infiltrated, and hair follicle necrosis. The mice in the THC group improvement in skin thickening, epidermal cells arranged neatly and loosely, and a few inflammatory cells were infiltrated compared to the UV group (Figure 3A). The above pathological results indicate that THC has a protective effect on the skin structure of photoaging mice.

In the UV group, the collagen fibers in the dermis showed disordered and irregularly distributed, with varying degrees of collagen fiber necrosis, nucleus consolidation and cytoplasmic light staining. However, the damaged were restored to a certain extent, and the collagen fibers in the dermis were more neatly arranged in the THC group (Figure 3B). The elastic fibers in the UV group showed breakage, degeneration, entanglement. After THC treatment, the elastic fibers showed elongated and orderly arrangement, partly interwoven, and partially restored mesh structure was visible (Figure 3C).

3.3. THC treatment affects SOD, HYP, MDA, GSH-Px expression

Level of SOD, GSH-Px, HYP were significantly increase (P < 0.05) and the level of MDA were significantly decrease (P < 0.01) in THC group compared with UV group, indicating that THC treatments effectively improves the antioxidant capacity of skin tissue, increases collagen content, and reduces peroxidation (Figure 4).

3.4. Overview mRNA sequencing

A total of 417,914,850 raw reads were generated, 139,007,364 in Ctrl group, 141,360,874 in UV group and 137,546,612 in THC group respectively. After cleaning out the unqualified reads and any other possible contaminants, 413,068,186 clean reads (134,804,378 in Ctrl
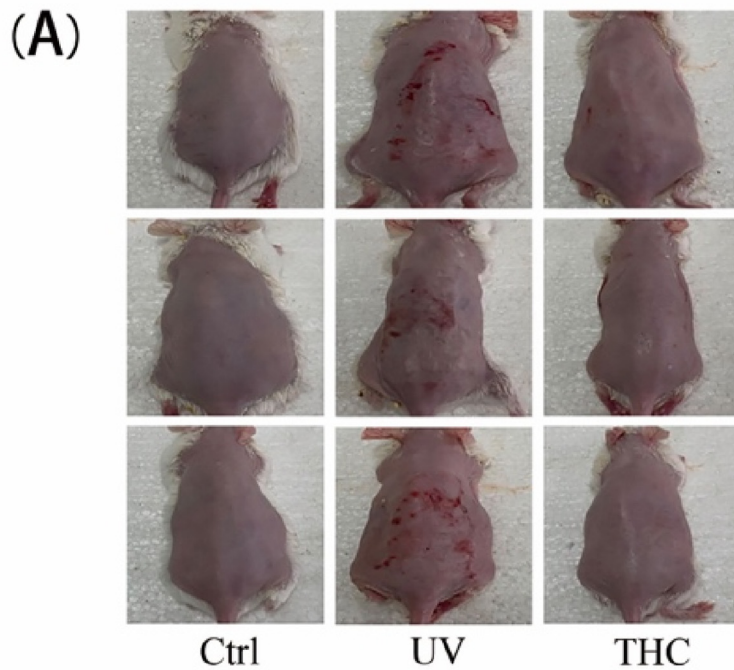
Figure 2. THC treatment improved photoaging appearance. Ctrl (control), UV(UVA + UVB), THC(UVA + UVB + THC THC100 mg/kg in 0.5% sodium carboxymethyl cellulose). (A) Photograph on the dorsal skin of KM mice at week 10 after indicated THC treatment and UVA irradiation. (B) Different group with equivalent UVA fluence radiation on photoaging was evaluated by Bissett scoring. Values presented are the means ± standard deviation (N = 12/group). *$P < 0.05$, **$P < 0.01$ Indicate compared to Ctrl group, compared to, #$P < 0.05$, ##$P < 0.01$ Indicate compared to UV group.
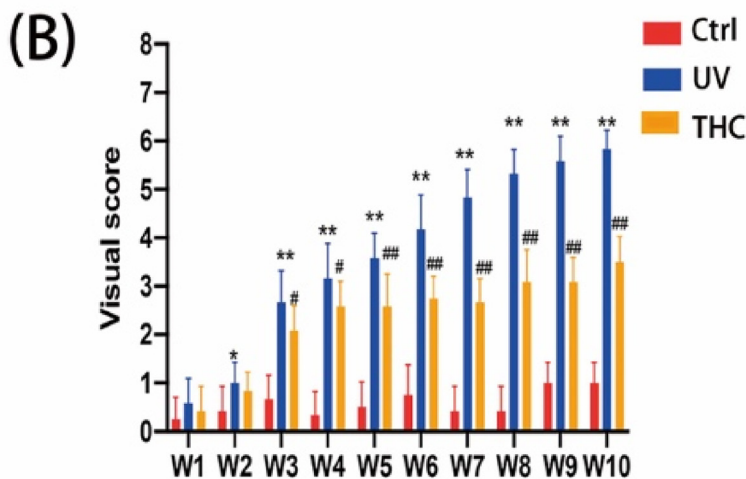
group, 136,097,408 in UV group, 132,166,400 in THC group) were determined.

The Q20, Q30, and GC contents of the clean reads were 97.64%, 93.10%, and 49.44%, respectively. The supplementary table S1 show us that each sample could meet the quality standards (Clean Bases > 12G, Error rate < 0.5, Q30 > 90%) which indicates high quality of the original data of RNA Sequencing for the subsequent bioinformatics analysis.

3.5. Altered mRNA profiles in Photoaging Mice Skins

A total of 54,532 mRNA transcripts identified by String Tie were estimated based on FPKMs. To determine the regulation of mRNA expression,

we performed an unsupervised clustering analysis of the significantly regulated genes ($p < 0.05$) in the skin of the Ctrl, UV and THC group (Figure 5A). Considering $p < 0.05$ and |log2 (fold change)| >1 as threshold, we obtained 29 differentially expressed mRNA transcripts in UV mice relative to Ctrl rats, including 18 up and 11 down-regulated transcripts (supplementary table S2). Meanwhile, 7 significantly dysregulated mRNAs were obtained in the THC group compared to the UV group, with 1 mRNA up-regulated and 6 mRNAs down-regulated (supplementary table S3). Veen analysis was additionally applied to lean the possible marker that participates in the exertion of THC ant-photoaging effect. We found three of them (Spink7, Edn3, Stab2) can be reversed by THC treatment in 18 up regulated genes following UV irradiation (Figure 5B).
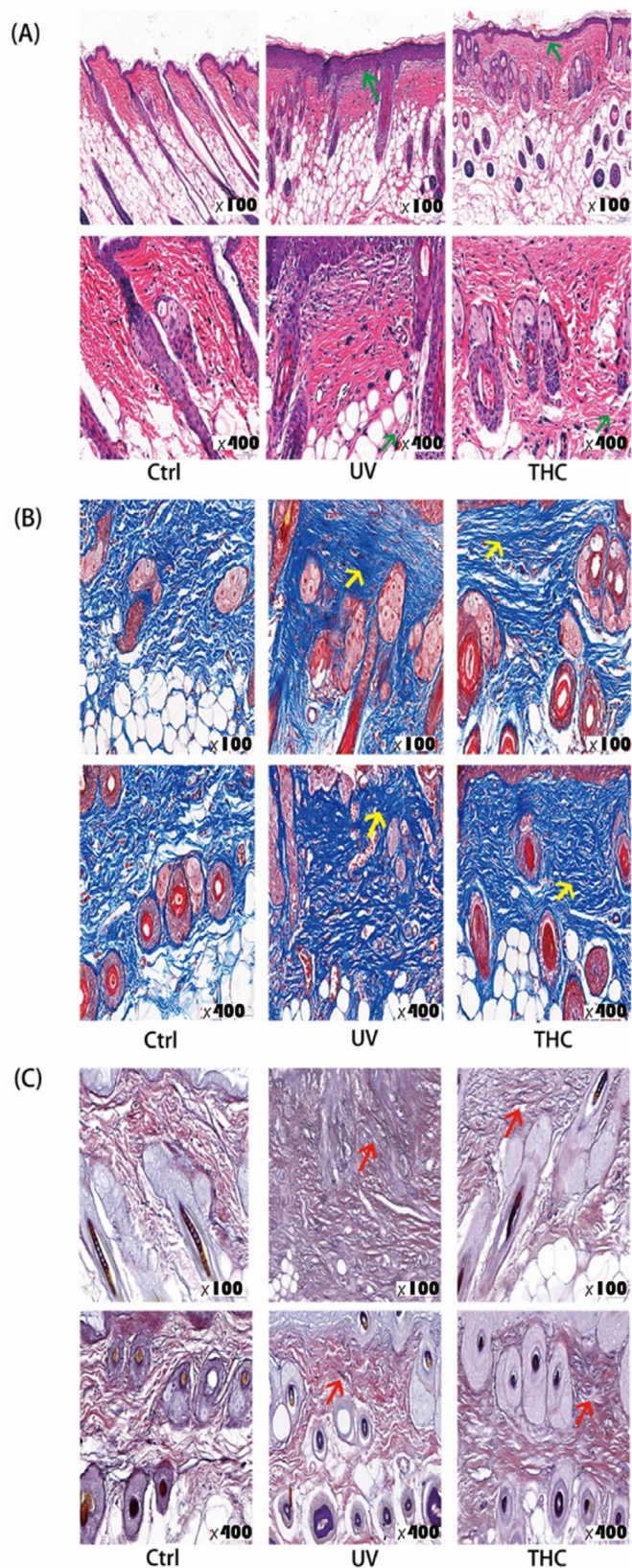
Figure 3. THC treatment improved skin tissue structure, collagen fibers and elastic fiber's structure (A) H & E (B) Masson's trichrome (C) Verhoeff prior. Ctrl (control group), UV (UVA + UVB group), THC (UVA + UVB + THC group THC100 mg/kg in 0.5% sodium carboxymethyl cellulose).

3.6. GO and KEGG pathway analyses of the mRNA

The GO enrichment analysis for the differentially expressed genes across three domains, including biological process (BP), cellular component (CC), and molecular function (MF), in this study we mainly focused on the biological process. A total of 166 terms were significantly enriched ($P < 0.05$), such as regulation of the skin muscle system and melanin biosynthesis process, the top 30 were drew Scatter plot (Figure- 6A). Besides , KEGG pathway analyses shows that the regulated genes were enriched in PPAR signaling pathway, MAPK signaling pathway, the top 20 were drew Dazzle (Figure 6B).

3.7. qRT-PCR Confirmation of Sequencing mRNAs

Six differentially expressed transcripts were randomly selected to confirm the accuracy and reliability of RNA sequencing using qRT-PCR. All selected mRNAs (Staf3, Spink7, Krt77, Edn3, Stab2, Rpl34) were exhibited significant different expressions (Figure 7A). The qRT-PCR results were consistent with the RNA-seq data in terms of the expression levels of the validated mRNAs.

Three target markers were further verified by qRT-PCR. Spink7, Edn3 and stab2 were significantly up-regulated after UV irradiation ($P < 0.01$) and down regulated after THC ($P < 0.01$), which was consistent with the results of high-throughput sequencing (Figure 7B).

4. Discussion

Skin is the outermost organ and the first line of defense in the human body, meanwhile, it also prone to aging due to external invasion [27]. UV radiation produces pro-inflammatory mediators and reactive oxygen species by reacting with DNA, destroys the skin regulation mechanism, and produces photoaging effects such as wrinkles, pigmentation and decreased skin firmness. THC, the natural antioxidants, early studies have shown that THC can improved extra cellular matrix components like collagen, elastin, and hyaluronic acid [28], it also have strong anti-oxidant activity and lipid peroxidation inhibition [29], so it can play an anti-aging role. In this study, we also confirmed the same anti-aging effect of THC, which can effectively reduce UV-induced damage such as epidermal thickening, wrinkles, erythema, and repair elastic and collagen fibers (Figure 2 and 3). Next, we tested anti-aging related indicators with ELISA, the result indicated that THC treatment increased the activity of antioxidant enzymes SOD and GSH-Px in photoaging rat, reduced the production of MDA, prevented peroxidation, and increased the content of HYP in the organism (Figure 5). Typical defense photoaging mechanisms against increase ROS in the skin include enzymes such as SODs, CAT, GPx and peroxiredoxins, and non-enzymatic antioxidants [30]. SOD plays an important role in defending against photo-oxidative stress, which has been attributed to the strong free radical scavenging activity of this enzyme.The activity of SOD can be used to reflect the free radical–scavenging ability and represents the antioxidant capacity of the organism [31]. GSH-Px, a peroxidase, can protect the organism from endogenously and exogenously induced lipid peroxidation [32]. Therefore, GSH-Px activity represents the antioxidant ability of the organism. Measurement of antioxidant activity (SOD, GSH-Px) in the skin of photodamaged mice provides insight into the extent of oxidative damage to the organism [33]. HYP content indirectly reflects collagen fibril change and a relatively stable amino acid. Generally, the level of HYP should be stable in the healthy state and this can be used to represent collagen levels and repair damaged skin tissue. Studies have indicated that exposure to UV radiation can reduce the concentration of hydroxyproline and activity of biotinidase and increased elastase activity, in the dorsal skin [34, 35]. Lipid peroxide is a product of the adverse effect of free radicals and is associated with the oxidative damage of cells caused by UV irradiation, which changes membrane fluidity and influences
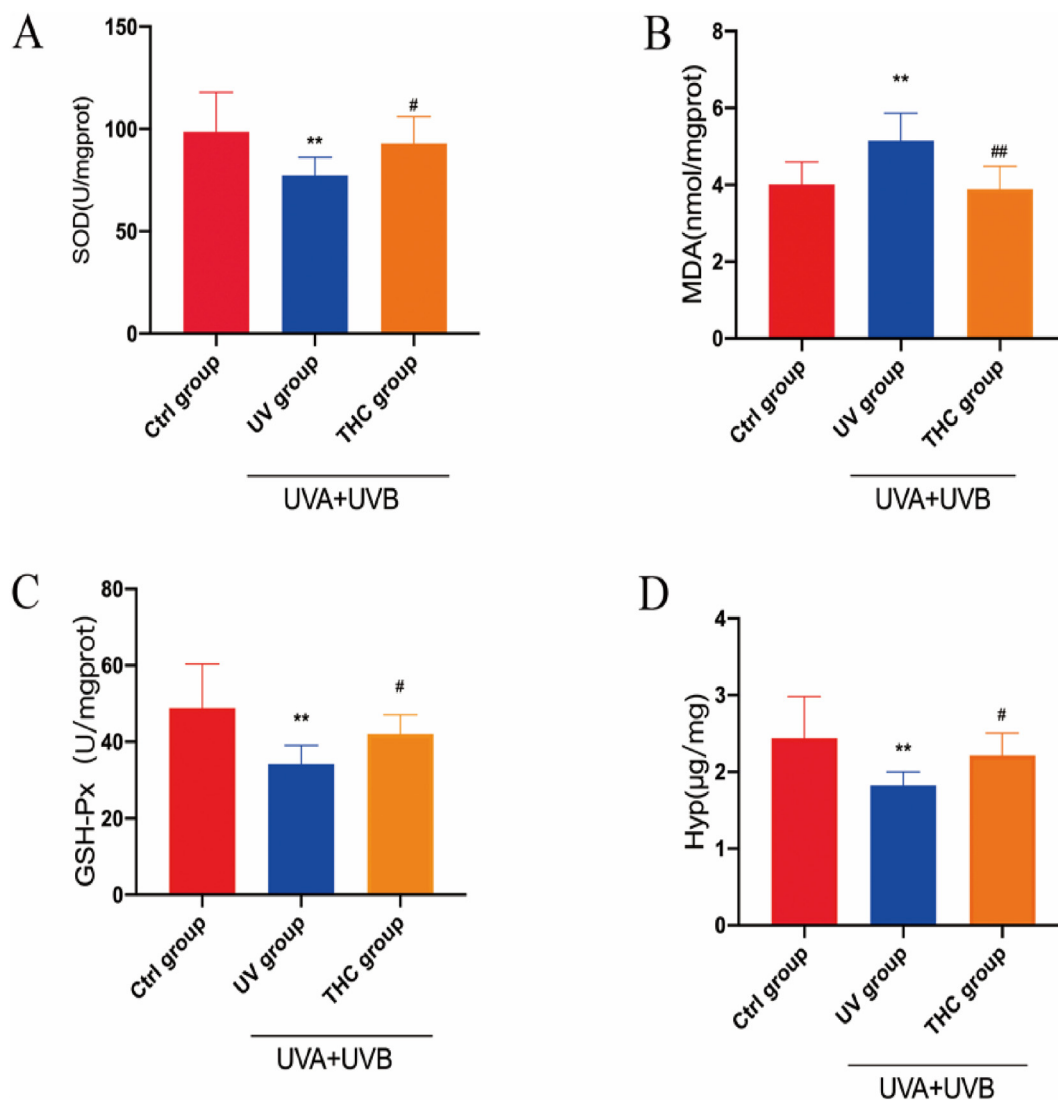
Figure 4. The detection results of SOD, MDA, GSH-Px and Hyp in mouse skin tissue. Ctrl group (control group), UV group (UVA + UVB group), THC group (UVA + UVB + THC group, THC100 mg/kg in 0.5% sodium Carboxymethyl cellulose).Values presented are the means ± standard deviation (N = 12/group). *$P < 0.05$, **$P < 0.01$ Indicate compared to Ctrl group, compared to, #$P < 0.05$, ##$P < 0.01$ Indicate compared to UV group.
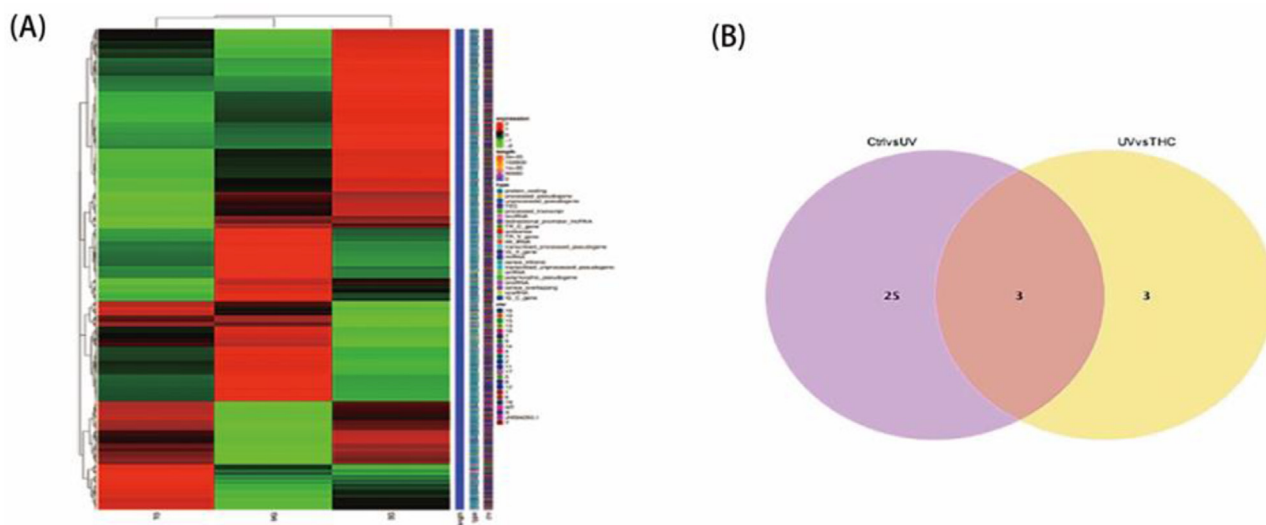

Figure 5. Altered mRNA profiles in Photoaging Mice Skins. BG (control group), MG (UVA + UVB group) TG (UVA + UVB + THC group, THC100 mg/kg in 0.5% sodium Carboxymethyl cellulose). (A)Heat map of significant mRNA (padj<0.05) from Ctrl and UV irradiated and THC treatment groups with green and red spectrum colors indicating down regulated and up regulated expression, respectively. (B)Venn diagrams shows overlaps of differentially expressed genes (padj<0.05 |log2 (fold change) | >1) between experimental groups. Three gene increased in UV group but decrease in THC group.
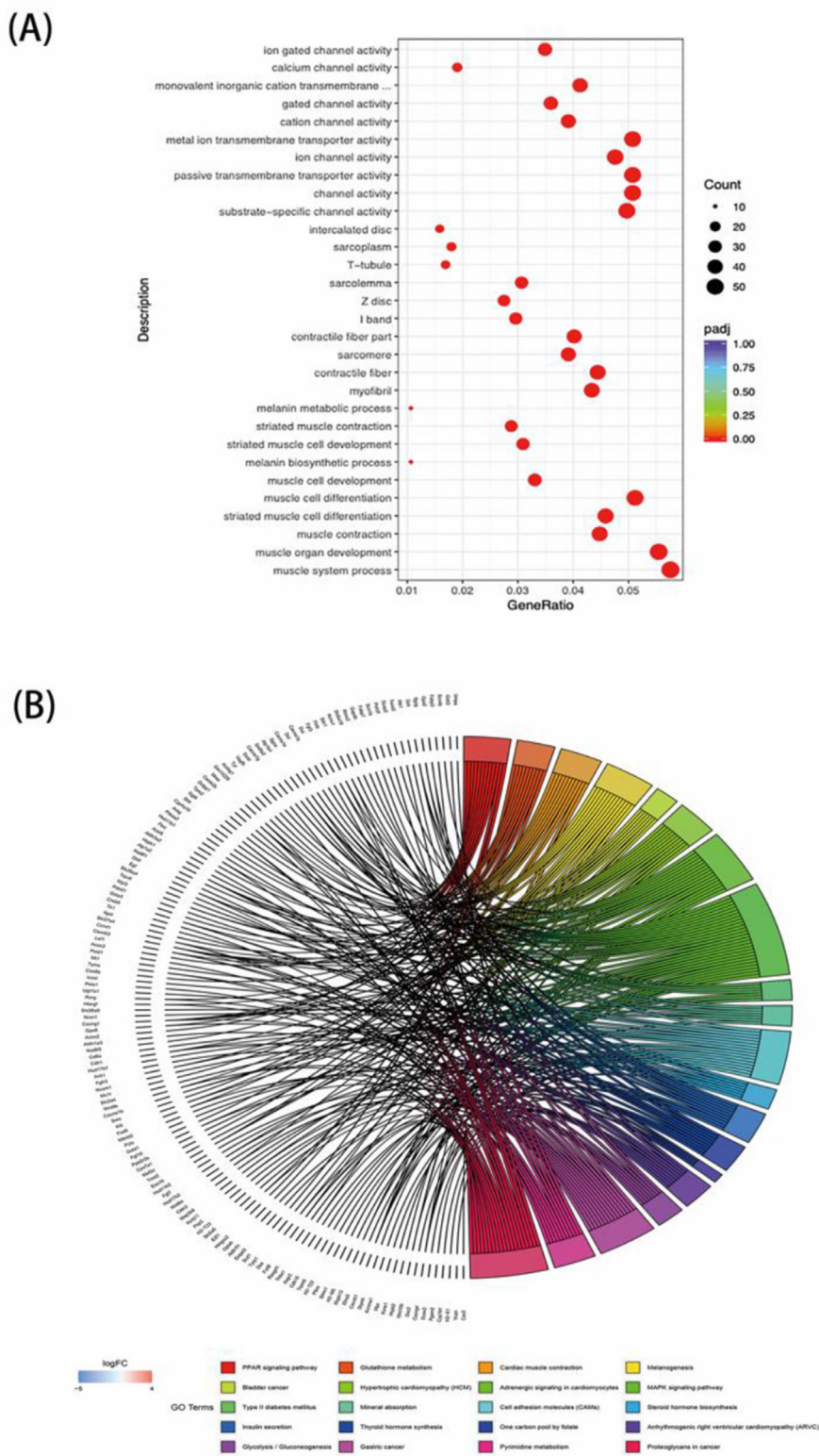
Figure 6. GO and KEGG Pathway Analyses of the mRNA. (A) Gene Ontology (GO) drew Scatter plot, the top 30 biological process were significantly enriched (P < 0.05). (B) KEGG Dazzle, the top 20 were significantly enriched (P < 0.05).

membrane protein activity [36], MDA is the major secondary metabolite of lipid peroxidation and is widely used as an indicator of cell membrane oxidative damage. Several studies have shown that THC has a significant inhibitory effect on lipid peroxidation in different models [37, 38]. Our results show that the skin changes caused by UV are consistent with previous studies, meanwhile, it confirmed that THC could inhibit the growth of free radicals, reduce lipid peroxidation and prevent ultraviolet induced aging.
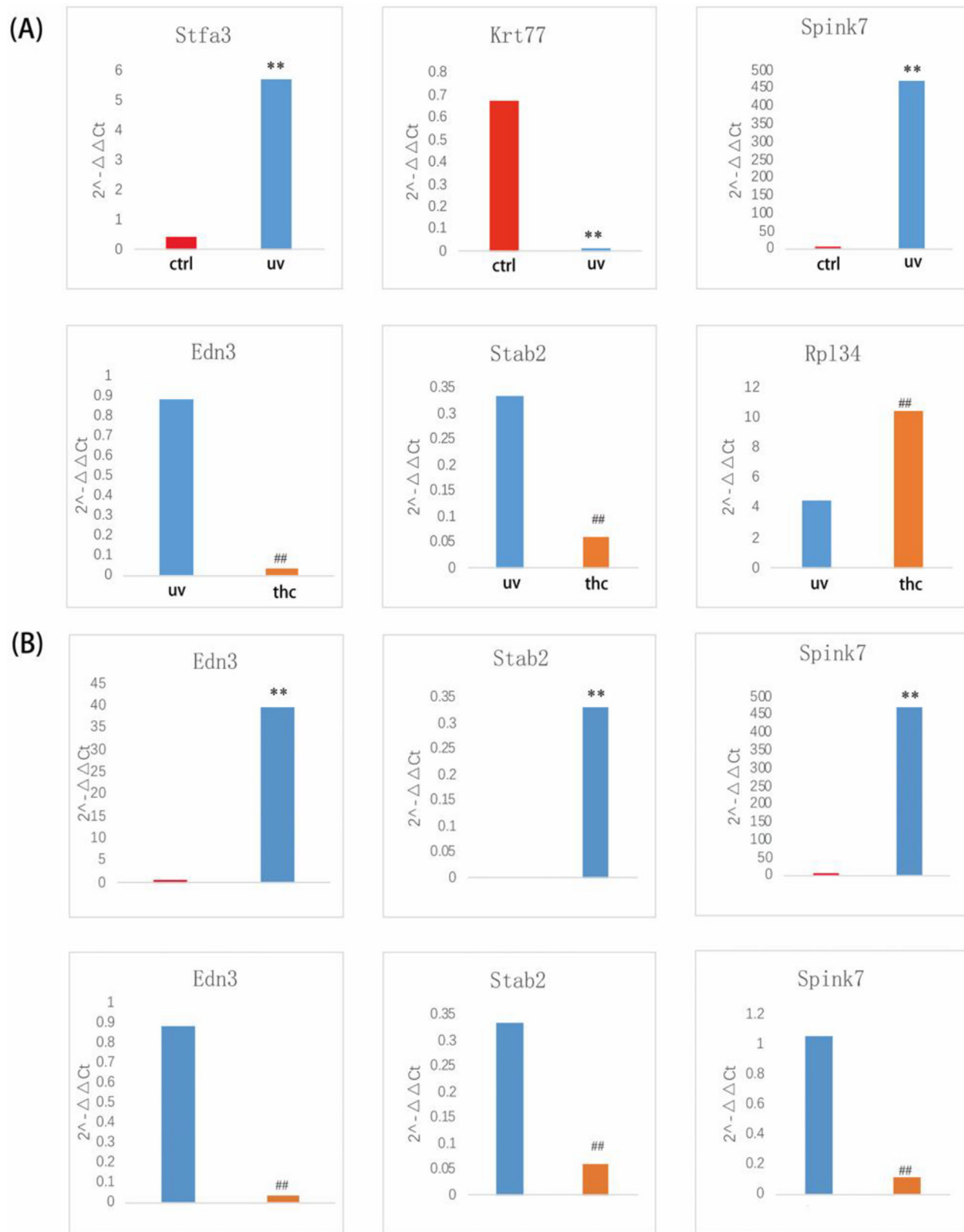
Figure 7. qRT-PCR Confirmation of Sequencing mRNAs. Ctrl (control group), UV group (UVA + UVB group), THC group (UVA + UVB + THC group, THC100 mg/kg in 0.5% sodium Carboxymethyl cellulose). (A) qRT-PCR showed that the result consistent with the RNA-seq data in terms of the expression levels of the validated mRNAs. (Red represents the blank control group, blue represents the model control group, and orange represents the tetrahydrocurcumin group, *P < 0.05, **P < 0.01). (B) qRT-PCR showed that Spink7, Edn3 and stab2 genes were significantly up-regulated after UV irradiation and down regulated after THC, which was consistent with the results of high-throughput sequencing (*P < 0.05, **P < 0.01).

Further we analysis the possible molecular mechanism of THC photoprotective effects, through the RNA-seq of skin tissue. We obtained 29 differentially expressed mRNA (18 up-regulated and 11 down-regulated, respectively) in UV group compare to Ctrl group and 7 differentially expressed mRNA in THC mice, among these 7, 6 were down-regulated and only 1 were up-regulated. The subsequent qRT-PCR data was

consistent with the RNA-seq assay, indicating that our resultant transcripts were of high quality. GO analysis of differentially expressed mRNA (P < 0.05) revealed that THC anti-skin aging were mainly associated with the regulation of biological process by muscle system process (GO:0003012), muscle contraction (GO:0006936), melanin biosynthetic process (GO:0042438). As for KEGG pathways analysis associated with the regulation of PPAR signaling pathway, Glutathione metabolism, Cardiac muscle contraction, Melanogenesis, MAPK signaling pathway mediate the progress of THC prevent skin photoaging.

From the differentially expressed genes, it can be seen that THC mainly caused the down regulation of mRNA, we compared the differential genes in two comparison groups, and found that Spink7, Edn3, Stab2 were co-expressed genes, which were significantly up-regulated in the skin tissues after UV irradiation and down-regulated after THC administration and in the subsequent PCR quantitative analysis of these three genes, it also showed the same change trend. Therefore, we speculate that spink7, Edn3, Stab2 are the key target gene for the action of THC. Spink7 is an important member of the SPINK family, which is associated with inflammatory diseases of the skin and other tissues. It has been shown that Spink7 expression is upregulated in inflammatory skin diseases such as psoriasis and eczema and play a role in skin homeostasis [39]. The anti-inflammatory effects of THC in the skin have been well studied , in vivo pharmacodynamics of THC administration decreased TNF-α, Nox2, Nox4, TNF-α and IL-6 levels [40, 41] , Our results show that THC can achieve anti-inflammatory effect by down regulating Spink7, which provides a new direction for the study of THC. Edn3 affects the migration and proliferation of melanocyte precursors and combine with growth factors to form mature melano-cytokines [42]. Long term exposure to ultraviolet radiation will make keratinocytes continuously secrete End1 and Edn3 and accelerate melanocyte proliferation and melanogenesis [43]. It has been demonstrated in previous cellular studies that THC have a good effect of anti-oxidation and anti-melanin production [28, 44]. This time, the same results were observed in our animal experiments. Stab2 acts as a scavenger of various hyaluronic acids (HA) [45, 46]. HA is present in large quantities in the extracellular matrix and in the skin and cartilage, and has good moisturizing and water-locking properties, which can effectively repair skin spreading [47, 48]. Previous in vitro studies have shown that THC can improved level of hyaluronic acid and inhabit melanin production [28], Now THC has the same effect from the RNA-seq results of rat skin. In conclusion, The down-regulated mRNA Spink7, Edn3 and Stab2 after THC intervention can prevent skin photoaging by reducing skin inflammatory reaction, melanin production and hyaluronic acid loss.

When the skin is subjected to photoaging, abnormal pigmentation occurs, leading to an increase in melanin, which causes pigmentation spots on the skin, and melanosis is an important manifestation of skin photoaging [49].With gradual aging of the skin, various factors such as lack of nutrients in skin tissues and decrease in collagen elastin make the balance tendency muscle degradation, resulting in skin muscle relaxation and eventually skin wrinkles [50].The results of the present study showed that the significantly different genes in the THC group were mainly enriched in the muscle system and melanin biosynthesis-related pathways, suggesting that the intervention of THC in skin photoaging may be related to the regulation of skin muscle and the regulation of melanin synthesis. We found that differentially expressed genes were most significantly enriched in the PPAR signaling pathway. The peroxisome proliferator-activated receptor PPAR has three main isoforms: PPARα, PPARβ, and PPARγ. Among them PPARγ plays an important role in regulating inflammation and oxidative stress, both by reducing inflammation by inhibiting downstream nuclear factor-κB (NF-κB) activation and by reducing oxidative stress by promoting protein kinase (AMPK) activation [51].

5. Conclusion

In conclusion, we elucidated the differential expression profiles of mRNAs in the skin of THC treated mice, our results indicated that THC shows a photoprotective effect against UV-induced skin damage, the mechanism of action is multi-channel and multi-target, the local skin effect is mainly through anti-inflammatory, improving extracellular matrix and inhibiting melanin production. Spink7, Edn3, Stab2 may be the potential biomarkers or therapeutic targets for THC prevention, PPAR signaling pathway may mainly signaling pathway.

Declarations

Author contribution statement

Chuan Xu: Conceived and designed the experiments; Performed the experiments; Analyzed and interpreted the data; Wrote the paper.

Xiao-Lu Li: Conceived and designed the experiments; Analyzed and interpreted the data.

Qian-Wei Xiong: Performed the experiments; Analyzed and interpreted the data; Wrote the paper.

YUE LI, Jun-Ning Zhao, Lu Zhang: Contributed reagents, materials, analysis tools or data.

Data availability statement

Data associated with this study [The RNA-seq] has been deposited at Gene Expression Omnibus database under the accession number SRP353684.

Declaration of interests statement

The authors declare no conflict of interest.

Additional information

Supplementary content related to this article has been published online at https://doi.org/10.1016/j.heliyon.2022.e09888.

References

[1] M. Cavinato, P. Jansen-Dürr, Molecular mechanisms of UVB-induced senescence of dermal fibroblasts and its relevance for photoaging of the human skin, Exp. Gerontol. 94 (2017) 78–82.

[2] A. Han, A.L. Chien, S. Kang, Photoaging, Dermatol. Clin. 32 (3) (2014) 291–299, vii.

[3] M. Ichihashi, H. Ando, The maximal cumulative solar UVB dose allowed to maintain healthy and young skin and prevent premature photoaging, Exp. Dermatol. 23 (Suppl 1) (2014) 43–46.

[4] E.C. De Fabo, Arctic stratospheric ozone depletion and increased UVB radiation: potential impacts to human health, Int. J. Circumpolar Health 64 (5) (2005) 509–522.

[5] A.V. Parisi, J. Turner, Variations in the short wavelength cut-off of the solar UV spectra, Photochem. Photobiol. Sci. 5 (3) (2006) 331–335.

[6] Z. Wu, L. Zhang, Polycomb group proteins: novel molecules associated with ultraviolet A-induced photoaging of human skin, Exp. Ther. Med. 14 (3) (2017) 2554–2562.

[7] C. Battie, et al., New insights in photoaging, UVA induced damage and skin types, Exp. Dermatol. 23 (Suppl 1) (2014) 7–12.

[8] E. Makrantonaki, et al., [Skin aging], MMW - Fortschritte Med. 155 Spec (2) (2013) 50–54, quiz 55.

[9] L. Baumann, How to use oral and topical cosmeceuticals to prevent and treat skin aging, Facial Plast Surg Clin North Am 26 (4) (2018) 407–413.

[10] M. Brennan, et al., Matrix metalloproteinase-1 is the major collagenolytic enzyme responsible for collagen damage in UV-irradiated human skin, Photochem. Photobiol. 78 (1) (2003) 43–48.

[11] P.A. Russo, G.M. Halliday, Inhibition of nitric oxide and reactive oxygen species production improves the ability of a sunscreen to protect from sunburn,

immunosuppression and photocarcinogenesis, Br. J. Dermatol. 155 (2) (2006) 408–415.

[12] L. Rittié, G.J. Fisher, Natural and sun-induced aging of human skin, Cold Spring Harb Perspect Med 5 (1) (2015) a015370.

[13] K. Jo, et al., An anthocyanin-enriched extract from vaccinium uliginosum improves signs of skin aging in UVB-induced photodamage, Antioxidants 9 (9) (2020).

[14] R. Yi, et al., Protective effects of Kuding Tea (Ilex kudingcha C. J. Tseng) polyphenols on UVB-induced skin aging in SKH1 hairless mice, Molecules 24 (6) (2019).

[15] R. Tundis, et al., Potential role of natural compounds against skin aging, Curr. Med. Chem. 22 (12) (2015) 1515–1538.

[16] A.R. Vaughn, A. Branum, R.K. Sivamani, Effects of turmeric (curcuma longa) on skin health: a systematic review of the clinical evidence, Phytother Res. 30 (8) (2016) 1243–1264.

[17] M. Kharat, et al., Physical and chemical stability of curcumin in aqueous solutions and emulsions: impact of pH, temperature, and molecular environment, J. Agric. Food Chem. 65 (8) (2017) 1525–1532.

[18] C.H. Park, et al., Neuroprotective effects of tetrahydrocurcumin against glutamate-induced oxidative stress in hippocampal HT22 cells, Molecules 25 (1) (2019).

[19] P. Murugan, L. Pari, Antioxidant effect of tetrahydrocurcumin in streptozotocin-nicotinamide induced diabetic rats, Life Sci. 79 (18) (2006) 1720–1728.

[20] K. Okada, et al., Curcumin and especially tetrahydrocurcumin ameliorate oxidative stress-induced renal injury in mice, J. Nutr. 131 (8) (2001) 2090–2095.

[21] V. Kakkar, et al., Topical delivery of tetrahydrocurcumin lipid nanoparticles effectively inhibits skin inflammation: in vitro and in vivo study, Drug Dev. Ind. Pharm. 44 (10) (2018) 1701–1712.

[22] A. Bhaskar Rao, et al., Wound healing: a new perspective on glucosylated tetrahydrocurcumin, Drug Des. Dev. Ther. 9 (2015) 3579–3588.

[23] M. Sumiyoshi, T. Hayashi, Y. Kimura, Effects of the nonsugar fraction of brown sugar on chronic ultraviolet B irradiation-induced photoaging in melanin-possessing hairless mice, J. Nat. Med. 63 (2) (2009) 130–136.

[24] R. Agrawal, I.P. Kaur, Inhibitory effect of encapsulated curcumin on ultraviolet-induced photoaging in mice, Rejuvenation Res. 13 (4) (2010) 397–410.

[25] D.L. Bissett, R. Chatterjee, D.P. Hannon, Photoprotective effect of topical anti-inflammatory agents against ultraviolet radiation-induced chronic skin damage in the hairless mouse, Photodermatol. Photoimmunol. Photomed. 7 (4) (1990) 153–158.

[26] S.Z. Kong, et al., Inhibitory effect of hydroxysafflor yellow a on mouse skin photoaging induced by ultraviolet irradiation, Rejuvenation Res. 16 (5) (2013) 404–413.

[27] J.H. Chung, Photoaging in asians, Photodermatol. Photoimmunol. Photomed. 19 (3) (2003) 109–121.

[28] M.K. Trivedi, et al., Protective effects of tetrahydrocurcumin (THC) on fibroblast and melanoma cell lines in vitro: it's implication for wound healing, J. Food Sci. Technol. 54 (5) (2017) 1137–1145.

[29] Y. Panahi, et al., Evidence of curcumin and curcumin analogue effects in skin diseases: a narrative review, J. Cell. Physiol. 234 (2) (2019) 1165–1178.

[30] S. Heydari, et al., Nanoethosomal formulation of gamma oryzanol for skin-aging protection and wrinkle improvement: a histopathological study, Drug Dev. Ind. Pharm. 43 (7) (2017) 1154–1162.

[31] S. Nanda, K. Madan, The role of Safranal and saffron stigma extracts in oxidative stress, diseases and photoaging: a systematic review, Heliyon 7 (2) (2021), e06117.

[32] R. Pandel, et al., Skin photoaging and the role of antioxidants in its prevention, ISRN Dermatol 2013 (2013), 930164.

[33] G.J. Fisher, The pathophysiology of photoaging of the skin, Cutis 75 (2 Suppl) (2005) 5–8. ; discussion 8-9.

[34] D. Cicek, et al., The protective effects of a combination of an arginine silicate complex and magnesium biotinate against UV-induced skin damage in rats, Front. Pharmacol. 12 (2021), 657207.

[35] A.C. Weihermann, et al., Elastin structure and its involvement in skin photoageing, Int. J. Cosmet. Sci. 39 (3) (2017) 241–247.

[36] J.E. Park, et al., Lipid peroxidation-mediated cytotoxicity and DNA damage in U937 cells, Biochimie 84 (12) (2002) 1199–1205.

[37] P. Anand, et al., Biological activities of curcumin and its analogues (Congeners) made by man and Mother Nature, Biochem. Pharmacol. 76 (11) (2008) 1590–1611.

[38] B.B. Aggarwal, L. Deb, S. Prasad, Curcumin differs from tetrahydrocurcumin for molecular targets, signaling pathways and cellular responses, Molecules 20 (1) (2014) 185–205.

[39] C. Weber, et al., The serine protease inhibitor of Kazal-type 7 (SPINK7) is expressed in human skin, Arch. Dermatol. Res. 309 (9) (2017) 767–771.

[40] J.E. Kim, et al., Tetrahydrocurcumin ameliorates skin inflammation by modulating autophagy in high-fat diet-induced obese mice, BioMed Res. Int. 2021 (2021), 6621027.

[41] K. Saini, et al., Tetrahydrocurcumin lipid nanoparticle based gel promotes penetration into deeper skin layers and alleviates atopic dermatitis in 2,4-dinitro-chlorobenzene (DNCB) mouse model, Nanomaterials 12 (4) (2022).

[42] D. Fang, et al., Defining the conditions for the generation of melanocytes from human embryonic stem cells, Stem Cell. 24 (7) (2006) 1668–1677.

[43] A.P. Benaduce, et al., Novel UV-induced melanoma mouse model dependent on Endothelin3 signaling, Pigment Cell Melanoma Res. 27 (5) (2014) 839–842.

[44] X. Tang, et al., Anti-melanogenic mechanism of tetrahydrocurcumin and enhancing its topical delivery efficacy using a lecithin-based nanoemulsion, Pharmaceutics 13 (8) (2021).

[45] N. Maeda-Smithies, et al., Ectopic expression of the Stabilin2 gene triggered by an intracisternal A particle (IAP) element in DBA/2J strain of mice, Mamm. Genome 31 (1-2) (2020) 2–16.

[46] Y. Hirose, et al., Inhibition of Stabilin-2 elevates circulating hyaluronic acid levels and prevents tumor metastasis, Proc. Natl. Acad. Sci. U. S. A. 109 (11) (2012) 4263–4268.

[47] R. Mota, et al., Skin adhesive versus subcuticular suture for perineal skin repair after episiotomy–a randomized controlled trial, Acta Obstet. Gynecol. Scand. 88 (6) (2009) 660–666.

[48] J.H. Oh, et al., Intrinsic aging- and photoaging-dependent level changes of glycosaminoglycans and their correlation with water content in human skin, J. Dermatol. Sci. 62 (3) (2011) 192–201.

[49] H. Woolery-Lloyd, J.N. Kammer, Treatment of hyperpigmentation, Semin. Cutan. Med. Surg. 30 (3) (2011) 171–175.

[50] H.M. Blau, B.D. Cosgrove, A.T. Ho, The central role of muscle stem cells in regenerative failure with aging, Nat. Med. 21 (8) (2015) 854–862.

[51] Y. Gao, R. She, W. Sha, Gestational diabetes mellitus is associated with decreased adipose and placenta peroxisome proliferator-activator receptor γ expression in a Chinese population, Oncotarget 8 (69) (2017) 113928–113937.